Effect of temperature and pre-annealing on the potential-induced degradation of silicon heterojunction photovoltaic modules

Jiaming Xu[1], Huynh Thi Cam Tu[1], Atsushi Masuda[2], Keisuke Ohdaira[1]

[1]*Japan Advanced Insistute of Science and Technology, Nomi, Ishikawa 923-1292, Japan*
[2]*Graduate School of Science and Technology, Niigata University, Niigata 950-2181, Japan*
E-mail: ohdaira@jaist.ac.jp

We investigate the effect of temperature and pre-annealing on the potential-induced degradation (PID) of silicon heterojunction (SHJ) photovoltaic (PV) modules. SHJ PV modules show a faster decrease in short-circuit current density (J_{sc}) at higher temperatures during PID tests. We also observe a complex relationship between the degree of the J_{sc} decrease and temperature during the PID tests. Pre-annealing before the PID tests at sufficiently high temperatures leads to the complete suppression of the PID of SHJ PV modules. The decrease in J_{sc} is known to be due to the chemical reduction of indium (In) in transparent conductive oxide (TCO) films in SHJ cells, in which water (H_2O) in SHJ modules is involved. These indicate that H_2O may out-diffuse from the SHJ PV modules during a PID test or pre-annealing at sufficiently high temperatures, by which the chemical reduction of indium in TCO into metallic In is suppressed.

Keywords: potential-induced degradation, photovoltaic module, silicon heterojunction solar cell, water

1. Introduction

Renewable energy has attracted much attention as one of the efficient solutions for global warming and energy problems. Photovoltaic (PV) systems, which can directly convert sunlight into electricity using solar cells, have been installed all over the world on a very large scale. In the large-scale PV systems, their high system voltage can cause potential-induced degradation (PID).[1–3] PID is a phenomenon which leads to significant performance loss in PV modules due to high voltage between an aluminum (Al) frame and solar cells. PID can occur in months or years, resulting in a significant power loss of the PV modules.

n-type crystalline silicon (c-Si) solar cells are expected to be widely used in the near future because they have a better conversion efficiency and less light-induced degradation compared to p-type c-Si solar cells.[4] To reduce the cost of electricity in the PV power plants using the n-type c-Si PV modules, not only an increase in the conversion efficiency of solar cells but an improvement in the long-term reliability, including the suppression of PID,[5–17] of PV modules is important. Si hetero-junction (SHJ) solar cells have shown a particularly high conversion efficiency as high as >25%.[18–21] However, there have been a few reports on the PID of SHJ PV modules.[22, 23]

We have thus far investigated the PID of SHJ PV modules.[24–28] Our previous investigations have revealed that SHJ PV modules show two-stage PID: the first-stage PID induces a decrease in short-circuit current density (J_{sc}) alone, while the second-stage PID is characterized by simultaneous decreases in J_{sc} and open-circuit voltage (V_{oc}). The first-stage PID is due to the formation of metallic indium (In) in a transparent conductive oxide (TCO) film and resulting loss in the optical transparency of TCO. The chemical reduction of In occurs by reacting with H generated by a reaction between sodium (Na) and water (H_2O).[27] The second-stage PID is induced by the introduction of Na ions drifting, for example, from the cover glass of the modules into Si and increased carrier recombination on the surface of c-Si. It should also be emphasized that the PID of SHJ PV modules becomes more severe if they receive a damp heat test prior to a PID test, and is strongly affected by H_2O in the module.[27] To understand the mechanism of the PID of SHJ PV modules in more detail and to clarify measures to suppress their PID, more systematic experiments under various conditions should be performed. In this study, we investigated the effects of temperature on the PID of SHJ PV modules. We also

investigated the effect of pre-annealing on their PID. In addition to our prior work,[28] we performed current density–voltage (*J–V*) measurement in the dark and external quantum efficiency (EQE) measurement, and discussed the influence of temperature during PID tests and pre-annealing in more detail.

2. Experimental Procedures

We used 20×20 mm^2-sized n-type rear-emitter SHJ cells cleaved from commercial n-type rear-emitter SHJ cells with tungsten-doped In_2O_3 (IWO) films as TCO on both sides with an area of 156×156 mm^2. Stacks consisting of cover glass (45×45×3.2 mm^3)/ethylene-vinyl acetate copolymer (EVA) sheet/SHJ cell/EVA/conventional backsheet (38-μm-thick poly(vinyl fluoride)/250-μm-thick poly(ethylene terephthalate)/38-μm-thick poly(vinyl fluoride)) were laminated to fabricate SHJ PV modules. The lamination was performed at a heater temperature of 150 °C both for evacuation (5 min) and for adhesion (16 min) processes. To avoid thermal damage to SHJ cells, we did not solder interconnector ribbons to the Ag electrodes of the SHJ cells; instead, the Ag electrodes and the interconnector ribbons were connected just by temporarily contacting each other and then by fixing them through the lamination. Note that this did not seriously degrade the fill factor (FF) of the *J–V* characteristics of SHJ PV modules, as shown below.

For the PID test of the SHJ PV modules, a negative voltage of −2000 V was applied using an insulation tester (TOS7210S, KIKUSUI) to an SHJ cell with respect to a grounded Al plate with a cell-sized hole put on the cover glass of the SHJ PV module.[29] Conductive rubber was inserted between the cover glass and the Al plate to improve their electrical contact. The electrodes on the front and rear sides of the SHJ cell were short-circuited in order to match their potentials. PID tests were conducted in air at various temperatures without intentional humidity stress (relative humidity <2%). Some of the SHJ modules received annealing prior to the PID test. The pre-annealing was performed at 85–110 °C for 3 days without bias stress. Note that the pre-annealing itself did not affect the performance of the SHJ PV modules. Dark and one-sun-illuminated *J–V* curves and EQE spectra of the SHJ PV modules were measured before and after the PID tests.

3. Results

3.1 Effect of temperature during the PID test

Figure 1 shows the dark and one-sun-illuminated *J–V* curves and EQE spectra of SHJ PV modules before and after the PID test at 85 °C. One can see a decrease in J_{sc} alone and almost no change in V_{oc} by the PID stress. No significant change in the dark *J–V* characteristics occurs, and EQE decreases in an entire wavelength region. These are the typical features of the first-stage PID of SHJ PV modules, the formation of metallic In and resulting reduction in the optical transparency of TCO.[24–26] Figure 2 shows the dark and one-sun-illuminated *J–V* curves and EQE spectra of SHJ PV modules before and after the PID test at 93 °C. Similar to the case of the PID test at 85 °C, J_{sc} reduction occurs in the first stage, followed by simultaneous reductions in J_{sc} and V_{oc} by continuing the PID test. The latter degradation is the second-stage PID of SHJ PV modules, which is due to the introduction of Na into Si and enhanced surface recombination of minority carriers. This is consistent with the change of the dark *J–V* curve and larger reduction in EQE in a shorter wavelength region, as shown in Figs. 2(a) and 2(c). These features reproduce our previous results.[24–26] Note that the second-stage PID occurs by the PID test at 85 °C in our previous PID test, whereas higher temperatures are needed for the emergence of the second-stage PID in this study. This difference may be due to the shape of an Al plate used for the PID tests.[24–26] Full-area Al plates were used in our previous PID tests, while the Al plates used in this study had a cell-size hole, which may result in less severe PID stress. The V_{oc} values shown in Figs. 1(b) and 2(b), ~0.7 V, are relatively small compared to reported values.[18,19] This is due to unpassivated edges of the cleaved cells, and gives no essential impact on the following discussion.

Figure 3 shows the J_{sc}, V_{oc}, FF, and maximum power (P_{max}), normalized by their initial values, of SHJ PV modules as a function of the duration of the PID tests at various temperatures from 70 to 100 °C. No remarkable change in FF is seen for all the SHJ PV modules, independent of temperature during PID tests. This is because a p^+ emitter locates on the rear side of the SHJ cells used in this study and the PID stress does not affect the p–n junction.[26] J_{sc} does not change by the PID test at 70 °C, while decreases more rapidly at higher temperatures. This is reasonable since the drift of Na towards the SHJ cells is accelerated at higher temperatures. Two-stage decreases in J_{sc} are seen in the SHJ PV modules that received the PID tests at 93 and 96 °C, and the second-stage decrease is accompanied by a reduction in V_{oc}, as shown in Fig. 3(b). This indicates the emergence

of the second-stage PID. Surprisingly, the PID test at 100 °C results in no V_{oc} reduction and less severe degradation of J_{sc} than the modules receiving a PID test at 93 and 96 °C.

3.2 Effect of pre-annealing

Figure 4 shows the normalized J_{sc} and V_{oc} of SHJ PV modules with and without pre-annealing at 110 °C as a function of PID-stress duration. The modules without pre-annealing show J_{sc} reductions, and the second-stage J_{sc} reduction, accompanied by a V_{oc} reduction, is also observed for the modules receiving a PID test at 96 °C. On the contrary, the modules with 3-days pre-annealing at 110 °C before the PID tests show no J_{sc} and V_{oc} reductions. This clearly indicates that pre-annealing is effective for the suppression of the first-stage and second-stage PID of SHJ PV modules. Figure 5 shows the normalized J_{sc} of SHJ PV modules without and with pre-annealing at various temperatures as a function of the duration of the PID test at 85 °C. The modules pre-annealed at 85 °C show the degradation of J_{sc} similar to those without pre-annealing. On the contrary, the modules pre-annealed at 93 and 110 °C show no reduction in J_{sc}. This suggests that a pre-annealing temperature is also a key to prevent the PID of SHJ PV modules.

4. Discussion

We first discuss the effect of temperature on the first-stage PID of SHJ PV modules. As shown in Fig. 3(a), the PID test at higher temperature leads to faster decrease in J_{sc}. This is quite reasonable since Na ions, one of the elements required for the chemical reduction of In in TCO, can drift towards the surface of an SHJ cell more rapidly at a higher temperature. On the other hand, the relationship between the degree of a decrease in J_{sc} and a temperature during a PID test is not straightforward: the PID test at the highest temperature (100 °C) does not result in the most severe degradation, even though the fastest Na drift is expected. We should thus consider other factors to understand this phenomenon.

The chemical reduction of In in TCO, which degrades the optical transparency of TCO and decreases J_{sc}, occurs by the following reactions.[27)]

$$Na + H_2O \rightarrow NaOH + H \quad (1)$$

$$In_2O_3 + 6H \rightarrow 2In + 3H_2O \quad (2)$$

According to these reactions, the formation of metallic In and resulting reduction in J_{sc} are related to H_2O inside the SHJ PV modules when the modules are fabricated. If H_2O inside the modules is eliminated, the chemical reduction of In in TCO may not occur and J_{sc} may not change, even if Na ions reach the surface of SHJ cells by the PID stress. Pre-annealing at sufficiently high temperatures may out-diffuse H_2O from the edges of the modules. This can also explain the seemingly peculiar dependence of the degree of PID on the temperature during the PID tests. The out-diffusion of H_2O can occur also during the PID test if the temperature is sufficiently high, and the out-diffusion of H_2O may overcome the acceleration of PID during the PID test at 100 °C.

We here discuss the out-diffusion of H_2O contained in EVA from the module edges more quantitatively. The diffusion coefficient of H_2O in EVA (D) has the following relationship with the absolute temperature T.

$$D = D_0 \exp(-E_D/kT) \quad (3),$$

where E_D is the activation energy of diffusion, D_0 is a frequency factor, and k is Boltzmann constant. Based on the values in Ref. 30, D_0=2.76 cm^2/s and E_D=0.4 eV, D values at 93 and 110 °C are 8.66×10^{-6} and 1.52×10^{-5} cm^2/s, respectively. Hence, the diffusion lengths L of H_2O during the pre-annealing at 93 and 110 °C for 3 days are estimated to be ~1.5 and ~2.0 cm using a relationship $L=(Dt)^{1/2}$, where t is a duration. These diffusion lengths are almost comparable to the half of the side length of the modules (2.25 cm), and the out-diffusion of H_2O during the pre-annealing seems to be possible, which supports our hypothesis.

We next consider the reason for the suppression of the second-stage PID of SHJ PV modules by the pre-annealing. The second-stage PID occurs by the introduction of Na into Si, and is seemingly not related to H_2O. The drift of Na ions does not occur in IWO because IWO is highly conductive and there is no electric field even under the PID stress. The movement of Na ions towards Si is thus based only on diffusion, and the diffusion of Na in IWO at ≤100 °C may be negligible. Once metallic In is formed in IWO based on the reaction of Eq. (2), IWO may become less dense due to the removal of O as H_2O, and

Na diffusion may be enhanced. That is, the mitigation of the first-stage PID may also lead to the suppression of the second-stage PID.

Finally, we discuss measures to the suppression of the PID of commercial SHJ PV modules. As is evident from the quantitative estimation of H_2O diffusion above, the out-diffusion of H_2O from the module edges by pre-annealing is not realistic for large-sized commercial modules. The important fact we found in this study is that the elimination of H_2O in encapsulant leads to the suppression of the PID of SHJ PV modules. The selection of encapsulant material, the optimization of the module lamination process, and the complete blocking of H_2O invasion during out-door operation may contribute to the reduction of H_2O absorption and resulting suppression of the PID of SHJ PV modules.

5. Conclusion

We investigated the effect of temperature and pre-annealing on the PID of SHJ PV modules. An increase in temperature during the PID test leads to more rapid decrease in J_{sc}. The PID test at 100 °C results in less significant degradation than those at 93–96 °C, and the modules pre-annealed at 93 and 110 °C do not show PID at all. These phenomena can be understood as the out-diffusion of H_2O from the edges of the SHJ PV modules. The results obtained in this study strongly suggest that the PID of SHJ PV modules can be completely suppressed if H_2O in the encapsulant of the modules is eliminated.

Acknowledgment

We would like to thank Assistant Professor Seira Yamaguchi of University of Tsukuba for his useful comments for this work. This work was supported by the New Energy and Industrial Technology Development Organization (NEDO).

References

1) W. Luo, Y. S. Khoo, P. Hacke, V. Naumann, D. Lausch, S. P. Harvey, J. P. Singh, J. Chai, Y. Wang, A. G. Aberle, and S. Ramakrishna, Energy Environ. Sci. **10**, 43 (2017), and references therein.
2) V. Naumann, D. Lausch, A. Hähnel, J. Bauer, O. Breitenstein, A. Graff, M. Werner, S. Swatek, S. Großer, J. Bagdahn, and C. Hagendorf, Sol. Energy Mater. Sol. Cells **120**, 383 (2014).
3) A. Masuda, M. Akitomi, M. Inoue, K. Okuwaki, A. Okugawa, K. Ueno, T. Yamazaki, and K. Hara, Curr. Appl. Phys. **16**, 1659 (2016).
4) A. ur Rehman and S. H. Lee, Sci. World J. **2013**, 470347 (2013).
5) R. Swanson, M. Cudzinovic, D. DeCeuster, V. Desai, J. Jürgens, N. Kaminar, W. Mulligan, L. Rodrigues-Barbosa, D. Rose, D. Smith, A. Terao, and K. Wilson, Ext. Abst. 15th Int. Photovoltaic Science and Engineering Conf., 2005, p. 410.
6) S. Bae, W. Oh, K. D. Lee, S. Kim, H. Kim, N. Park, S.-Il Chan, S. Park, Y. Kang, H.-S. Lee, and D. Kim, Energy Sci. Eng. **5**, 30 (2017).
7) A. Halm, A. Schneider, V. D. Mihailetchi, L. J. Koduvelikulathu, L. M. Popescu, G. Galbiati, H. Chu, and R. Kopecek, Energy Procedia **77**, 356 (2015).
8) J. Šlamberger, M. Schwark, B. B. Van Aken, and P. Virtič, Energy **161**, 266 (2018).
9) W. Luo, P. Hacke, S. M. Hsian, Y. Wang, A. G. Aberle, S. Ramakrishna, and Y. S. Khoo, IEEE J. Photovolt. **8**, 1168 (2018).
10) K. Hara, S. Jonai, and A. Masuda, Sol. Energy Mater. Sol. Cells **140**, 361 (2015).
11) S. Yamaguchi, A. Masuda, and K. Ohdaira, Sol. Energy Mater. Sol. Cells **151**, 113 (2016).
12) Y. Komatsu, S. Yamaguchi, A. Masuda, and K. Ohdaira, Microelectron. Reliab. **84**, 127 (2018).
13) S. Yamaguchi, K. Nakamura, A. Masuda, and K. Ohdaira, Jpn. J. Appl. Phys. **57**, 122301 (2018).
14) K. Ohdaira, Y. Komatsu, T. Suzuki, S. Yamaguchi, and A. Masuda, Appl. Phys. Express **12**, 064004 (2019).
15) T. Suzuki, S. Yamaguchi, K. Nakamura, A. Masuda, and K. Ohdaira, Jpn. J. Appl. Phys. **59**, SCCD02 (2020).

16) Y. Xu, A. Masuda, and K. Ohdaira, Jpn. J. Appl. Phys. **60**, SBBF08 (2021).
17) S. Yamaguchi, B. B. Van Aken, M. K. Stodolny, J. Löffler, A. Masuda, and K. Ohdaira, Sol. Energy Mater. Sol. Cells **226**, 111074 (2021).
18) D. Adachi, J. L. Hernández, and K. Yamamoto, Appl. Phys. Lett. **107**, 233506 (2015).
19) X. Ru, M. Qu, J. Wang, T. Ruan, M. Yang, F. Peng, W. Long, K. Zheng, H. Yan, and X. Xu, Sol. Energy Mater. Sol. Cells **215**, 110643 (2020).
20) K. Yoshikawa, H. Kawasaki, W. Yoshida, T. Irie, K. Konishi, K. Nakano, T. Uto, D. Adachi, M. Kanematsu, H. Uzu, and K. Yamamoto, Nat. Energy **2**, 17032 (2017).
21) K. Yamamoto, K. Yoshikawa, H. Uzu, and D. Adachi, Jpn. J. Appl. Phys. **57**, 08RB20 (2018).
22) Z. Xiong, T. M. Walsh, and A. G. Aberle, Energy Proc. **8**, 384 (2011).
23) O. A. Arruti, L. Gnocchi, F. Lisco, A. Virtuani, and C. Ballif,, Proc. 37th European Photovoltaic Solar Energy Conf. Exhib., 2020, p. 789.
24) S. Yamaguchi, C. Yamamoto, K. Ohdaira, and A. Masuda, Sol. Energy Mater. Sol. Cells **161**, 439 (2017).
25) S. Yamaguchi, C. Yamamoto, K. Ohdaira, and A. Masuda, Prog. Photovolt. **26**, 697 (2018).
26) S. Yamaguchi, C. Yamamoto, Y. Ohshita, K. Ohdaira, and A. Masuda, Sol. Energy Mater. Sol. Cells **216**, 110716 (2020).
27) A. Masuda, C. Yamamoto, Y. Hara, S. Jonai, Y. Tachibana, T. Toyoda, T. Minamikawa, S. Yamaguchi, and K. Ohdaira, Jpn. J. Appl. Phys. **59**, 076503 (2020).
28) J. Xu, H. T. C. Tu, A. Masuda, and K. Ohdaira, Ext. Abst. 2021 Int. Conf. Solid State Devices and Materials (SSDM2021), 2021, F-5-02, p. 345.
29) K. Hara, H. Ichinose, T. N. Murakami, and A. Masuda, RSC Adv. **4**, 44291 (2014).
30) M. D. Kempe, Sol. Energy Mater. Sol. Cells **90**, 2720 (2006).

Figure Captions

Fig. 1 (Color online) (a) Dark *J–V* curves, (b) one-sun-illuminated *J–V* curves, and (c) EQE spectra of an SHJ PV module before and after the PID test at 85 °C.

Fig. 2 (Color online) (a) Dark *J–V* curves, (b) one-sun-illuminated *J–V* curves, and (c) EQE spectra of an SHJ PV module before and after the PID test at 93 °C.

Fig. 3 (Color online) (a) J_{sc}, (b) V_{oc}, (c) FF, and (d) P_{max}, normalized by their initial values, of SHJ PV modules as a function of the duration of the PID tests at various temperatures.

Fig. 4 (Color online) (a) J_{sc} and (b) V_{oc}, normalized by their initial values, of SHJ PV modules with and without annealing at 110 °C prior to the PID test as a function of the duration of PID tests at 85 and 96 °C.

Fig. 5 (Color online) Normalized J_{sc} of SHJ PV modules without and with pre-annealing at various temperatures as a function of the duration of the PID test at 85 °C.

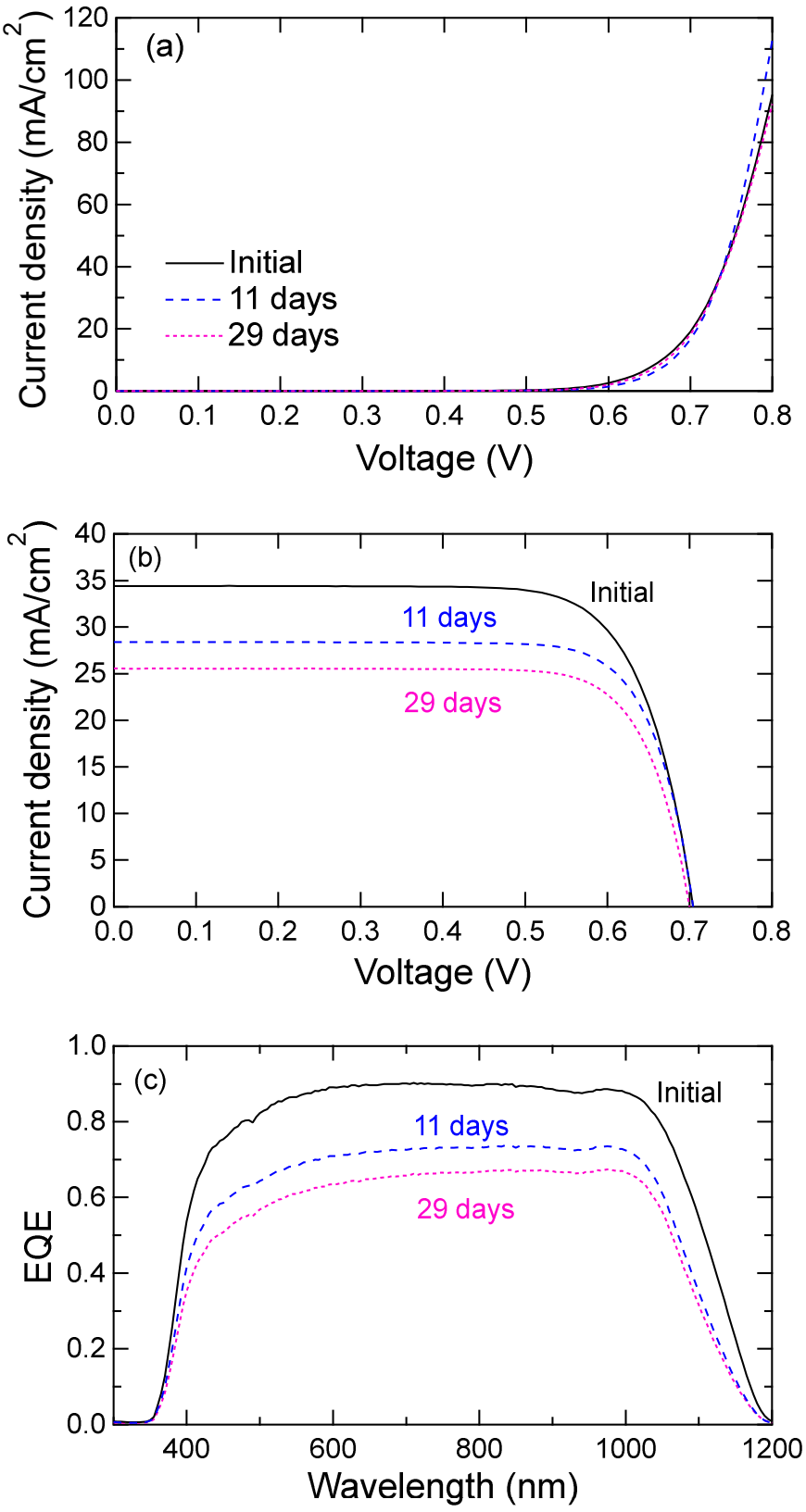

Fig. 1 J. Xu et al.,

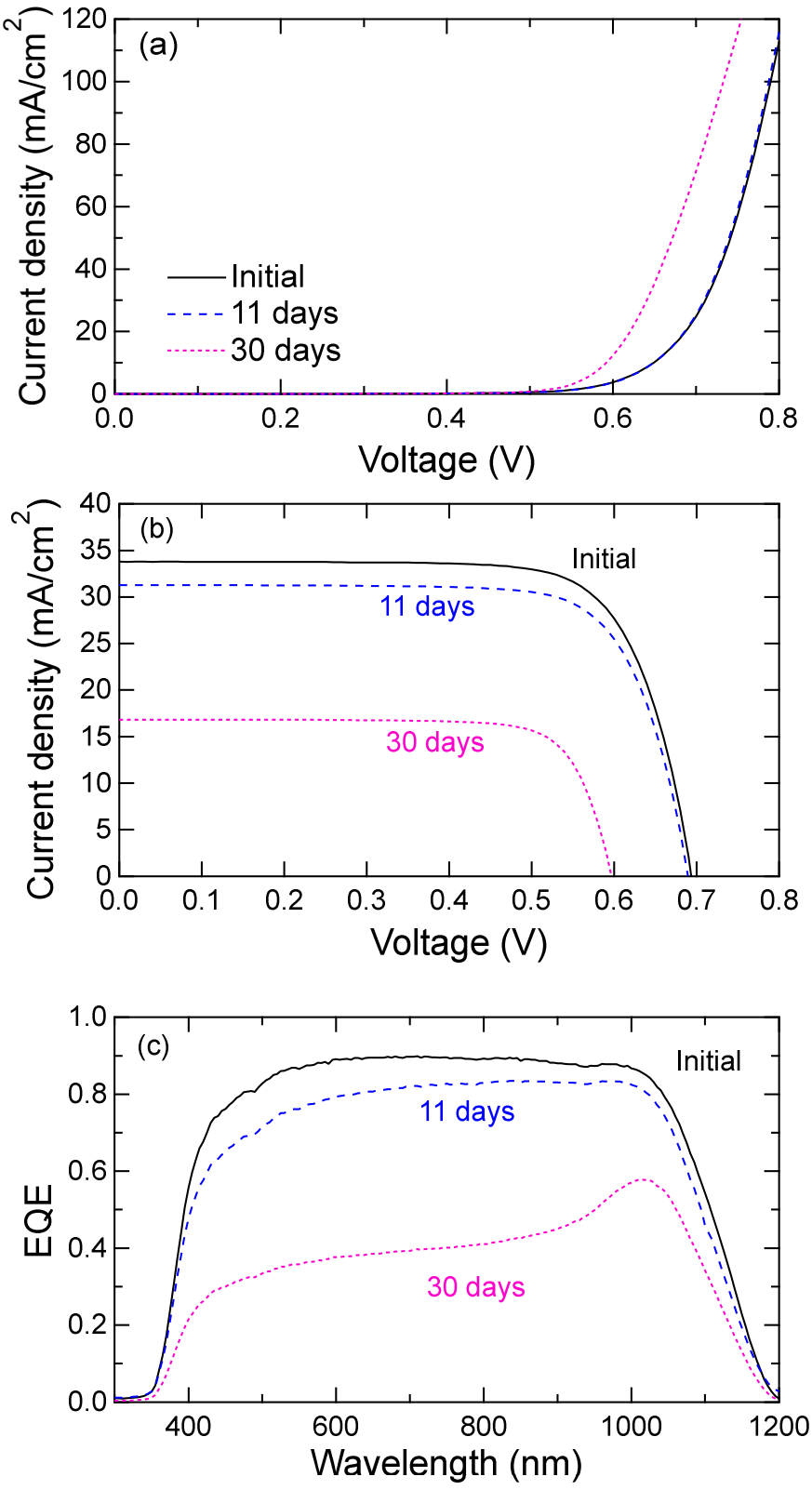

Fig. 2 J. Xu et al.,

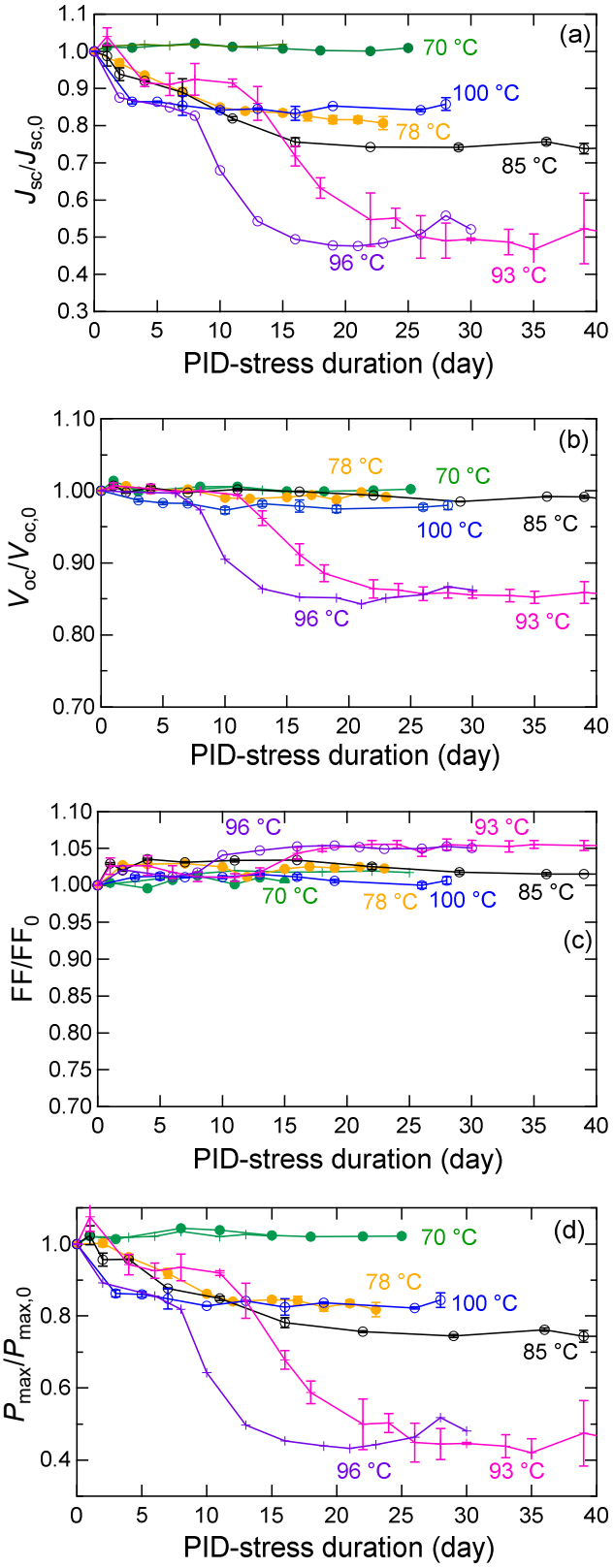

Fig. 3 J. Xu et al.,

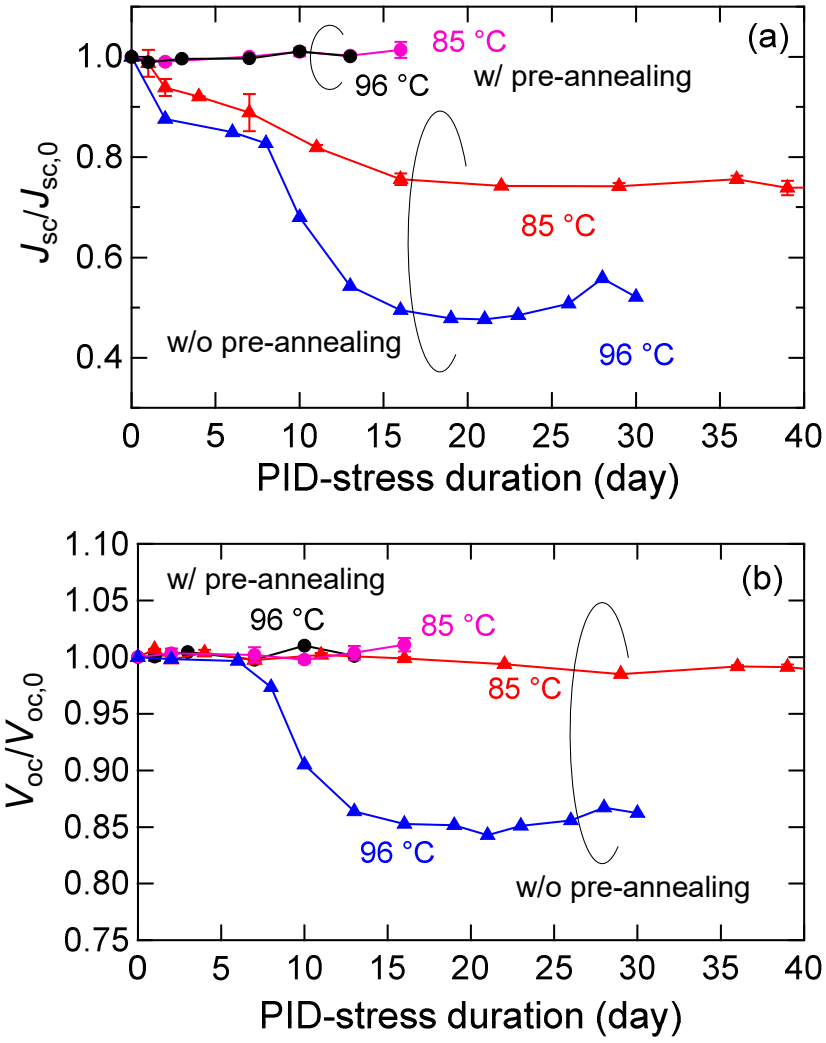

Fig. 4 J. Xu et al.,

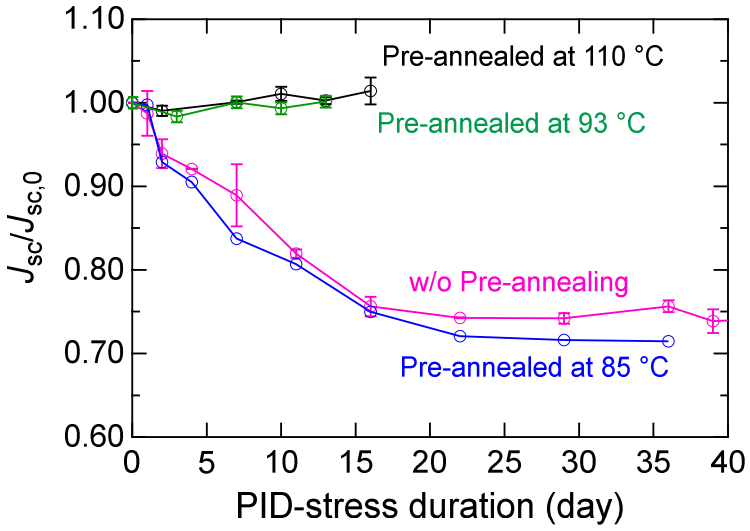

Fig. 5 J. Xu et al.,